

Band Crossing and Novel Low-Energy Behaviour in a Mean Field Theory of a Three-Band Model on a $Cu-O$ lattice

D. I. Golosov*, A. E. Ruckenstein[†], and M. L. Horbach[‡]

Department of Physics, Rutgers University, Piscataway, NJ 08855-0849, U.S.A.

We study correlation effects in a three-band extended Hubbard model of Cu-O planes within the $1/N$ mean field approach, in the infinite U limit. We investigate the emerging phase diagram and discuss the low energy scales associated with each region. With increasing direct overlap between oxygen orbitals, $t_{pp} > 0$, the solution displays a band crossing which, for an extended range of parameters, lies close to the Fermi level. In turn this leads to the nearly nested character of the Fermi surface and the resulting linear temperature dependence of the quasi-particle relaxation rate for sufficiently large T . We also discuss the effect of band crossing on the optical conductivity and comment on the possible experimental relevance of our findings.

PACS numbers: 71.10.Fd, 71.10.Hf, 71.27+a, 71.30+h

Typeset Using *REVTEX*

*Present address: The James Franck Institute, The University of Chicago, 5640 S. Ellis Avenue, Chicago, IL 60637, U. S. A.

[†]Also at: Institut für Theorie der Kondensierten Materie, Universität Karlsruhe, 76132 Karlsruhe, Germany.

[‡]Present address: Information Builders, 1250 Broadway, New York, NY 10001, U. S. A.

A number of versions of the extended three-band Hubbard models have been studied recently [1–5] with the expectation that they are relevant to the physics of the high- T_c cuprates. The complexity of these models leads to a broad spectrum of phenomena, from metal-to-insulator transitions, charge and spin-density waves and superconductivity to more mundane single particle band-structure effects. Most of the studies searched for novel low-energy excitations which would explain the departures from Landau’s Fermi Liquid phenomenology implicit in many of the experimental results in the normal state of the cuprates.

In the simplest discussions based on mean field theories of strongly correlated Fermi systems such non-Fermi liquid behaviour occurs above some small energy scale, T_{coh} . Already within the three-band models there are a number of different physical mechanisms resulting in the appearance of small energy scales, namely the proximity of the chemical potential to a van Hove singularity in the single-particle density of states [6], heavy Fermion behaviour [4] and the Brinkman-Rice metal-to-insulator transition [4,5,7], and the effects of strong anti-ferromagnetic spin fluctuations in the paramagnetic state [7,8].

In this letter we focus on a band-crossing which arises upon hole doping ($n_0 > 1$) for values of the $O - O$ hopping matrix elements larger than a filling-dependent critical value, $t_{pp}^c > 0$. In the vicinity of $t_{pp} = t_{pp}^c$ the lowest (*Cu*-like) band is only weakly dispersing along the Brillouin zone boundary leading to a nearly one dimensional “extended” van Hove singularity in the density of states (cf. Ref. [9]). In addition, once the doping is increased to a particular concentration, $n_0 = n_{cr}$, the band-crossing occurs *at* the Fermi level. (This rare situation in the context of three dimensional band-metals is best exemplified by the self-intersecting Fermi surface of graphite [10].) Moreover, at n_{cr} , the resulting Fermi surface (FS) is perfectly nested with an incommensurate nesting wave vector. A special feature of this situation is that the nearly nested character of the Fermi surface survives for a wide range of dopings around n_{cr} . In particular, in the vicinity of n_{cr} the resulting low-energy scale varies with doping slower ($T_{coh} \propto (n_0 - n_{cr})^2$) than that expected from the saddle-point van Hove scenario ($\propto -|n_0 - n_{cr}| / \ln |n_0 - n_{cr}|$).

We emphasize that in the experimentally interesting case of hole doping, the band-

crossing only occurs for a particular sign of $t_{pp}(> 0)$. Under these conditions the van Hove singularity of the density of states does not scan the Fermi level with increasing doping and thus the van Hove mechanism discussed in [6] cannot be realized. Since, generically, the crossing of two eigenvalues of a hermitian operator requires the fine tuning of three real parameters [11] band-crossing in two-dimensions is typically avoided. Our situation is special as the mean field Hamiltonian can be reduced to a real matrix and thus crossing may occur through the tuning of only two parameters (e.g., the two components of the momentum, (k_x, k_y)). We note that avoided crossing along a line in 2-dimensions (or at a point in 1-D) is responsible for the heavy Fermion regime of our mean field solution [12].

In the present paper, we concentrate on the model with $t_{pp} > 0$. We note that this choice disagrees with the situation which apparently takes place in all the cuprates, where the estimates extracted from LDA calculations [13,14] imply that t_{pp} is negative. In YBCO near optimal doping the corresponding FS agrees qualitatively with the ARPES results [15]. Some questions however arose in the context of BiSCO where two sheets appear in one of the earlier interpretations of the photo-emission results [16] and there remains controversy of whether the origin of the two sheets is a lattice superstructure effect, bilayer splitting or some other effect. The main reason for studying a model with $t_{pp} > 0$ is the fact that, as we will see shortly, a rich array of many-body and single-particle phenomena arise in a natural way. It is interesting, however, that in some cases one is able to draw a parallel between our results and the experimental observations. If this model has any relevance it can only be so due to strong correlations which are believed to be crucial to the physics of the cuprates [17] and are not properly accounted for within the LDA. To exemplify this point, imagine starting with a $t_{pp} = 0$ tight binding model with a large value of the Hubbard U and deriving an effective low-energy Hamiltonian by “integrating out” charge fluctuations on the Cu -sites one obtains an effective $O - O$ hopping amplitude which changes sign with increasing U . In the $U \rightarrow \infty$ limit this yields $t_{pp}^{eff} > 0$ (cf. Ref. [18]).

Our starting point is the extended three-band Anderson-Hubbard Hamiltonian describing the interaction between the oxygen p_x, p_y ($P_{x\sigma}, P_{y\sigma}$) and copper $d_{x^2-y^2}$ (d_σ) orbitals. As

depicted in Fig. 1, the Hamiltonian includes the direct hopping of electrons between oxygen sites (t_{pp}) and a hybridization between copper and oxygen orbitals (t_{pd}). Apart from the Hubbard repulsion at the copper sites – here after taken as infinite – we also take into account the nearest neighbor Coulomb interaction, V , between copper and oxygen. The infinite Hubbard repulsion is incorporated through the replacement of the original copper orbitals operators, d_σ , by the projected Fermion operators, $\tilde{d}_\sigma = d_\sigma(1 - n_{-\sigma})$ which eliminate double occupancy at the copper sites; here $n_{\sigma'} = d_{\sigma'}^\dagger d_{\sigma'}$ is the local number operator for the orbital with spin σ' . Below we treat this Hamiltonian by a simple mean field (Hartree-Fock) approximation: as explained in Refs. [5,19], the factorization of the equations of motion requires a generalization of the usual Wick's theorem. The resulting mean field equations can be adequately described by the quasi-particle Hamiltonian,

$$\begin{aligned} \mathcal{H}_{MF} = & -2it'_{pd} \sum_{\vec{k}, \sigma} \tilde{d}_\sigma^\dagger(\vec{k}) \left[\sin \frac{k_x}{2} P_{x\sigma}(\vec{k}) - \sin \frac{k_y}{2} P_{y\sigma}(\vec{k}) \right] - 4t_{pp} \sum_{\vec{k}, \sigma} P_{x\sigma}^\dagger(\vec{k}) P_{y\sigma}(\vec{k}) \sin \frac{k_x}{2} \sin \frac{k_y}{2} + h.c. \\ & + (\epsilon'_d - \mu) \sum_{\vec{k}, \sigma} \tilde{d}_\sigma^\dagger(\vec{k}) \tilde{d}_\sigma(\vec{k}) + (\epsilon'_p - \mu) \sum_{\vec{k}, \sigma} [P_{x\sigma}^\dagger(\vec{k}) P_{x\sigma}(\vec{k}) + P_{y\sigma}^\dagger(\vec{k}) P_{y\sigma}(\vec{k})]. \end{aligned} \quad (1)$$

Here $t'_{pd} = \sqrt{1 - n_d}(t_{pd} + V\lambda/8t_{pd})$, $\epsilon'_d = \epsilon_d + \lambda + 4n_p V$ and $\epsilon'_p = \epsilon_p + 2n_d V$ are renormalized values of the hybridization amplitude, and local energy levels of the copper and oxygen orbitals, $t_{pd}, \epsilon_d, \epsilon_p$, respectively; given $\Delta^{(0)} = \epsilon_p - \epsilon_d$ and the total filling, $n_0 = n_d + 2n_p$, the values of the local copper (n_d) and oxygen (n_p) occupancy, the energy shift, λ , and the chemical potential, μ , are to be determined self-consistently from the mean field equations (MFE),

$$n_0 = \frac{2}{N} \sum_{\vec{k}} \sum_{i=1}^3 n_F(\epsilon_i(\vec{k}) - \tilde{\mu}), \quad (2)$$

$$n_d = \frac{2}{N} \sum_{\vec{k}} \sum_{i=1}^3 n_F(\epsilon_i(\vec{k}) - \tilde{\mu}) \frac{(\epsilon_i(\vec{k}) - \Delta)^2 - 16t_{pp}^2 \sin^2 \frac{k_x}{2} \sin^2 \frac{k_y}{2}}{\prod_{j \neq i} (\epsilon_i(\vec{k}) - \epsilon_j(\vec{k}))}, \quad (3)$$

$$\lambda = -\frac{8}{N} \sqrt{\frac{2}{1 - n_d}} t_{pd} t'_{pd} \sum_{\vec{k}} \sum_{i=1}^3 n_F(\epsilon_i(\vec{k}) - \tilde{\mu}) \frac{4t_{pp} \sin^2 \frac{k_y}{2} + \epsilon_i(\vec{k}) - \Delta}{\prod_{j \neq i} (\epsilon_i(\vec{k}) - \epsilon_j(\vec{k}))} \sin^2 \frac{k_x}{2} \quad (4)$$

where $\tilde{\mu} = \mu - \epsilon'_d$, $\Delta = \epsilon'_p - \epsilon'_d$, N is the number of copper sites, and $n_F(x) = [\exp \beta x + 1]^{-1}$ is the Fermi-Dirac distribution function. Finally, the quasi-particle energies, $\omega_i(\vec{k}) = \epsilon'_d + \epsilon_i(\vec{k})$,

$i = 1 \div 3$, should be determined from the cubic secular equation for $\epsilon_i(\vec{k})$, namely,

$$\begin{aligned} \epsilon^3 - 2\Delta \epsilon^2 + \left[\Delta^2 - 4t_{pd}^2 \left(\sin^2 \frac{k_x}{2} + \sin^2 \frac{k_y}{2} \right) - 16t_{pp}^2 \sin^2 \frac{k_x}{2} \sin^2 \frac{k_y}{2} \right] \epsilon + \\ + 4\Delta t_{pd}^2 \left(\sin^2 \frac{k_x}{2} + \sin^2 \frac{k_y}{2} \right) - 32t_{pd}^2 t_{pp} \sin^2 \frac{k_x}{2} \sin^2 \frac{k_y}{2} = 0. \end{aligned} \quad (5)$$

Equations (2–5) define the filling-dependent bandstructure. The no-double occupancy constraint manifests itself through two important effects: (i) the upward shift of the copper-like band and (ii) its associated band narrowing. The first occurs as a result of the no double occupancy constraint which forces the copper component of the lower band to lie within a hybridization width of the chemical potential; while the band narrowing is due to the $\sqrt{1-n_d}$ factor multiplying t_{pd} and reflects the fact that coherent hybridization involves rare charge fluctuations at the copper sites. The interplay between these correlation effects and the band structure leads to the rich phase diagram shown in Figs. 2. To summarize the possible behaviours imagine starting with the bare copper level below the oxygen level, $\Delta^{(0)} > 0$ and increasing the filling from $n_0 = 0$. We will consider the $\Delta^{(0)}$ vs. n_0 plane for two qualitatively different cases, $t_{pp} < t_0$ and $t_{pp} > t_0$, where $t_0 = \sqrt{\alpha_1}|t_{pd}| + \alpha_2 V$ with the two constants given by $\alpha_1 = (4\sqrt{2} - 5)/\pi \approx .21$ and $\alpha_2 = [\pi - 4(\sqrt{2} - 1)]/4\pi \approx .12$. In each case we single out three $\Delta^{(0)} = \text{const}$ cuts, denoted by A, B , and C in the figures. For $t_{pp} < t_0$ and for small values of $\Delta^{(0)}$ (cut A in Fig. 2a) one starts with conventional metallic behaviour for $n_0 \ll 1$. Below half filling one then scans the the chemical potential through the van Hove singularity (saddle point) switching from hole-like to electron-like FS. The situation at $n_0 < 1$ is reminiscent of what would happen at $n_0 > 1$ if we reverse the sign of the oxygen-oxygen hopping. The low energy scale is provided by the difference between the Fermi level and the saddle point energy (see fig.3), and although in the case of the Fermi energy equal to ϵ_{vHs} one does get the linear temperature dependence of the quasiparticle relaxation rate [6], the corresponding crossover temperature T_* above which the relaxation rate becomes linear in T is in this case expected to scale as $(n_0 - n_{vHs})/\ln|n_0 - n_{vHs}|$ [20], where n_{vHs} is the value of filling corresponding to $\tilde{\mu} = \epsilon_{vHs}$. The physical consequences of the presence of a small energy scale $\tilde{\mu} - \epsilon_{vHs}$ have been discussed in the literature in great

detail [21].

With further increasing n_0 the chemical potential scans through another van Hove singularity associated with the bottom of the lower oxygen-like band, which, at $T = 0$, causes a negative jump in the compressibility, $dn_0/d\mu$. Above this doping concentration, $dn_0/d\mu < 0$, and the system is thermodynamically unstable with respect to phase separation. Within the region of instability, the absolute value of the (negative) compressibility increases and, at some point, diverges. The compressibility then changes sign and the system enters a normal metallic phase with large and rapidly decreasing value of the compressibility.

The shape of the unstable region is highly sensitive with respect to the parameters of the Hamiltonian. The phase separation would be circumvented altogether in the presence of a real long-ranged Coulomb interaction. Beyond half-filling the bottoms of the two lowest bands coincide (“tangency”) beyond which a crossing of the *Cu*- and lower *O*-like bands (conic point) emerges. At sufficiently large filling the chemical potential scans through the band crossing energy. Along cut B in Fig. 2a a new feature arises at $n_0 = 1$ (between the two van Hove singularities), namely the Brinkman-Rice metal-to-insulator transition (BRT) where the copper-like band becomes completely flat (see below). Finally, along cut C, in addition to the BRT, a heavy fermion regime with exponentially small $1 - n_d$ and a conic band crossing point below the chemical potential appears immediately above half filling, extends over a finite range of dopings and then terminates via a smooth crossover into a conventional metal. In the case of cut C, the phase separation region is located above this crossover. In the metallic phase, the conic point eventually crosses the chemical potential. For $t_{pp} > t_0$ both van Hove singularities and the tangency appear already below half filling. The only other qualitative difference from the $t_{pp} < t_0$ case is the possible appearance of reentrant heavy fermion behaviour below the BRT critical value of $\Delta^{(0)}$ (see cut B in Fig. 2b). Numerical calculations show that the features of the phase diagram persist at finite temperature, with the value of $\Delta^{(0)}$ decreasing as temperature increases. We are now in position to discuss these features in more detail.

The mean-field bandstructure is characterized by three energy scales, namely the band-

width of the lower band, the difference $\tilde{\mu} - \epsilon_{vHs}$ between the Fermi level and the van Hove singularity (corresponding to the saddle point in the lowest band dispersion) and the difference between the Fermi level and the energy $\epsilon_{cr} = -t'_{pd}/t_{pp}$ of the band crossing point. The values of these three quantities, computed along the three cuts A, B, and C of fig. 2a are plotted in fig. 3. One can see, that indeed the lowest energy scale in the metallic phase above half filling over an extended range of dopings is provided by $\tilde{\mu} - \epsilon_{cr}$, which vanishes at some particular filling $n_{cr}(\Delta^{(0)})$ and at small values of $|n_0 - n_{cr}| \ll 1$ depends linearly on filling, $\tilde{\mu} - \epsilon_{cr} \propto n_{cr} - n_0$.

The FSs that emerge when the Fermi level lies close to ϵ_{cr} are shown in Fig. 4 [22]. It is a striking feature of the present model that when the band crossing occurs exactly at the Fermi level, the FS is formed by the straight lines $k_x = k_{cr}$ and $k_y = k_{cr}$ (with $k_{cr} = \pi - \pi n_{cr}/4$), and is therefore perfectly nested along the coordinate axes. It is well-known [23] that in such a situation the quasiparticle relaxation rate becomes linear in temperature. One can therefore expect that as the value of filling approaches n_{cr} , the quasiparticle relaxation rate undergoes a crossover to the linear temperature dependence; this is also the case when, at some fixed value of n_0 , temperature increases beyond certain crossover value T_* .

The simplest way to exemplify this behaviour is to replace the nested parts of the FS by two nearly straight segments of length L and curvature radius $R \gg L$, also assuming that the velocities of quasiparticles on these segments are equal to v and antiparallel to each other. One can then estimate the contribution of these segments to the off-shell decay rate due to a weak interparticle contact interaction, $U\delta(\vec{r} - \vec{r}')$. For $\omega > vL^2/R$, and when momentum vector \vec{p} lies at the middle of the straight segment of the FS, the decay rate is linear in frequency, $\text{Im}\Sigma(\omega, \vec{p}) \approx (3U^2L^2\omega)/(16\pi^3v^2)$ whereas at very low frequencies, $\omega \ll vL^2/R$, one gets

$$\text{Im}\Sigma(\omega, \vec{p}) \approx \frac{RU^2}{(2\pi v)^3} \left[2\omega^2 \ln \frac{vL^2}{\omega R} - \frac{1}{3}\omega^2 \right]. \quad (6)$$

The finite-temperature on-shell quasiparticle relaxation rate can be estimated by substituting $T \rightarrow \omega$ in these expressions. The quantity L^2/R measures the deviation of the nearly-flat

segments of the Fermi surface from the tangent straight lines and provides a new low-energy scale, vL^2/R . As expected [23], for values of $\omega, T \gg vL^2/R$ $\text{Im}\Sigma$ is proportional to $x = \max\{\omega(>0), T\}$, whereas at low energies the behaviour reduces to the 2D Fermi Liquid result $\text{Im}\Sigma \propto -x^2 \ln x$ [24].

For our mean field band structure $R \propto (\tilde{\mu} - \epsilon_{cr})^{-2}$ in the limit of $|\tilde{\mu} - \epsilon_{cr}/\tilde{\mu}| \ll 1$ and $L \sim \pi$. Since $\tilde{\mu} - \epsilon_{cr} \propto n_{cr} - n_0$, it follows that the crossover scale $T^* = vL^2/R \propto (n_0 - n_{cr})^2$. As a result, the linearity of the relaxation rate survives over a wider range of dopings than in the van Hove scenario for which $T_{vh}^* \propto |(n_0 - n_{cr})/\ln(n_0 - n_{cr})|$.

Let us now take a closer look of the band crossing point. Expanding the dispersion law about this point leads to the following two branches,

$$\epsilon_{1,2}(\vec{k}) = A(\vec{k}) \mp \sqrt{B(\vec{k})(k_x + k_y - 2k_{cr})^2 - C(\vec{k})(k_x - k_y)^2}, \quad (7)$$

where A, B and C are smooth functions of momentum \vec{k} . Note that the square-root behaviour in (7) is associated with the non-analytic behaviour of the matrix elements of the unitary transformation which diagonalizes the mean field Hamiltonian; more precisely, the limiting values of these coefficients at $\vec{k} \rightarrow \vec{k}_{cr}$ depend on the direction of approach. This affects, for example, the interband matrix element of the quasi-particle position operator which diverges at the crossing point as $\vec{r}_{12}(\vec{k}) \propto (\epsilon_1(\vec{k}) - \epsilon_2(\vec{k}))^{-1}$. On the other hand, the corresponding interband matrix element of the velocity operator $\vec{v}_{12} = (d\vec{r}/dt)_{12} = i(\epsilon_1 - \epsilon_2)\vec{r}_{12}$ remains finite at $\vec{k} \rightarrow \vec{k}_{cr}$ but its limiting values still depend on the direction of approach. In turn, the leading interband contribution to the optical conductivity (ignoring all quasi-particle interactions) [25],

$$\text{Re}\sigma_{\alpha\beta}^{12} = \frac{e^2}{2\pi\omega} \int v_{12}^\alpha(\vec{k})v_{21}^\beta(\vec{k}) \left[n_F(\epsilon_1(\vec{k})) - n_F(\epsilon_2(\vec{k})) \right] \delta(\epsilon_1(\vec{k}) - \epsilon_2(\vec{k}) + \omega) d^2k, \quad (8)$$

(the indices α, β take values x or y) displays an anomaly associated with the peculiar behaviour of \vec{v}_{12} in the presence of band crossing. The integration in (8) leads to the result sketched in fig. 5. Note the presence of two square-root singularities in the frequency derivative of the conductivity: one at the threshold frequency

$$\omega_t = 2 \frac{t_{pd}^2 + t_{pp}\Delta}{3t_{pd}^2 + 2t_{pp}\Delta} |\mu - \epsilon_{cr}|, \quad (9)$$

below which $\text{Re}\sigma_{\alpha\beta}^{12}(\omega)$ is equal to zero, and another at $\omega'_t = \omega_t \cdot (3t_{pd}^2 + 2t_{pp}\Delta)/t_{pd}^2$. These singularities originate from the tangency between the ellipse $\epsilon_2(\vec{k}) = \epsilon_1(\vec{k}) + \omega$ and the two borders of the stripe $\tilde{\mu} < \epsilon_1(\vec{k}) < \tilde{\mu} + \omega$. At larger frequencies, $\omega \gg \omega_t, \omega'_t$ (but ω still much smaller than the bandwidths), $\text{Re}\sigma^{12}(\omega)$ approaches a constant value. Finally, if the band crossing occurs precisely at the Fermi level, the independence of $\text{Re}\sigma_{12}(\omega)$ on frequency survives down to $\omega = 0$. It is amusing to note the resemblance of the threshold behaviour in Fig. 5 with the “mid-infrared peak” observed in optical conductivity experiments [26]. Within this scenario the weak doping dependence of the “peak” position could only be accounted for if the system is sufficiently far below the critical filling, n_{cr} .

It is easy to see that the value of the threshold frequency and the nature of singularities at $\omega = \omega_t, \omega'_t$ is in fact unaffected by the RPA corrections. The latter, in principle, might add excitonic features to the profile of $\text{Re}\sigma_{\alpha\beta}(\omega)$ (delta-functional peaks below the threshold or Lorentzian peaks above the threshold). We have checked, however, that excitonic bound states do not occur for physically relevant interaction strengths ($V < W^2/\omega_t$, where W is the conduction electron bandwidth). Also, the effects of resonances above threshold is small for $\omega \sim \omega_t$. Thus, at frequencies of the order of ω_t RPA modifies the rigid-band result by a factor of order unity.

We close by noting that when the Fermi level lies in the vicinity of a band crossing point, one should be able to observe the phenomenon of *magnetic breakdown* [27], namely, the restructuring of the FS that takes place at sufficiently high magnetic fields through the tunneling of electrons between different FS sheets. This phenomenon and its consequences for magneto-transport in weak fields in the presence of a conic point will be described elsewhere [28].

We take our pleasure in thanking R. J. Gooding, M. I. Kaganov, and I. E. Trofimov for stimulating and enlightening discussions. This work was supported in part by ONR Grant # N00014-92-J-1378.

REFERENCES

- [1] K. Levin, J. H. Kim, J. P. Lu, and Q. Si, *Physica* **C175**, 449 (1991).
- [2] G. Kotliar, P. A. Lee, and N. Read, *Physica* **C153–155**, 538 (1988).
- [3] J. H. Kim, K. Levin and A. Auerbach, *Phys. Rev.* **B39**, 11633 (1989).
- [4] M. Grilli, B. G. Kotliar and A. J. Millis, *Phys. Rev.* **B42**, 329 (1990).
- [5] J. C. Hicks, A. E. Ruckenstein and S. Schmitt-Rink, *Phys. Rev.* **B45**, 8185 (1991).
- [6] D. M. Newns, H. R. Krishnamurthy, P. C. Pattnaik, C. C. Tsuei, C. C. Chi, and C. L. Kane, *Physica* **B186**, 801 (1993), and references therein.
- [7] S. Carpara and M. Grilli, *Phys. Rev.* **B49**, 6971 (1994).
- [8] Q. Si, Y. Zha, and K. Levin, *Phys. Rev.* **B47**, 9055 (1993);
- [9] A. A. Abrikosov, J. C. Campuzano and K. Gofron, *Physica* **C214**, 73 (1993). Q. Si, *Int. J. Mod. Phys.* **B8**, 47 (1994), and references therein.
- [10] J. C. Slonczewski and P. R. Weiss, *Phys. Rev.* **109**, 272 (1958).
- [11] J. von Neumann and E. P. Wigner, *Physik. Zeitschr.* **30**, 467 (1929).
- [12] See Ref. [4] for a treatment of 1D case.
- [13] M. S. Hybertsen, E. B. Stechel, M. Schluter, D. R. Jennison, *Phys. Rev.* **B41**, 11068 (1990).
- [14] O. K. Andersen, A. I. Liechtenstein, O. Jepsen and F. Paulsen, *J. Phys. Chem. Solids* **56**, 1573 (1995).
- [15] Z.-X. Shen and D. S. Dessau, *Phys. Rept.* **253**, 1 (1995), and references therein.
- [16] D. Dessau *et al.*, *Phys. Rev. Lett.* **71**, 2781 (1993).
- [17] P. W. Anderson, *in*: Strong Correlation and Superconductivity, eds H. Fukuyama, S.

- Maekawa and A. P. Malozemoff (Springer, Tokyo) 1989.
- [18] see, for example, D. M. Frenkel, R. J. Gooding, B. I. Shraiman, and E. D. Siggia, Phys. Rev. **B41**, 350 (1990).
- [19] A. E. Ruckenstein and S. Schmitt-Rink, Phys. Rev. **B38**, 7188 (1988).
- [20] S. Gopalan, O. Gunnarson, O. K. Anderson, Phys. Rev. **B46**, 11798 (1992).
- [21] M. L. Horbach and H. Kajüter, Int. Journal Mod. Phys. **B9**, 1067 (1995); R. S. Markiewicz, preprint (1996), and references therein.
- [22] It is interesting to note the resemblance of this FS to the one proposed for Sr_2RuO_4 . The band structure calculations for Sr_2RuO_4 seem to suggest the occurrence of band crossing near the Fermi energy (see T. Oguchi, Phys. Rev. **B51**, 1385 (1995); D. J. Singh, Phys. Rev. **B52**, 1358 (1995); A. P. Mackenzie *et al.*, Phys. Rev. Lett. **76**, 3786 (1996)).
- [23] A. Virosztek and J. Ruvalds, Phys. Rev. **B42**, 4064 (1990).
- [24] C. Hodges, H. Smith and J. W. Wilkins, Phys. Rev. **B4**, 302 (1971).
- [25] The analysis of the behaviour of the expression (8) for the case when the FS has points of self-intersection (due to the band crossing) in 3D has been carried out by M. I. Kaganov and I. M. Lifshitz (Sov. Phys. JETP **18**, 655 (1964)).
- [26] D. B. Tanner and T. Timusk, *in*: Physical properties of high temperature superconductors, Vol. 3, D. M. Ginsberg, ed. (World Scientific, Singapore, 1992), p.338, and references therein.
- [27] M. I. Kaganov and A. A. Slutzkin, Physics Reports **98**, 189 (1983), and references therein.
- [28] D. I. Golosov and A. E. Ruckenstein, in preparation.

FIGURES

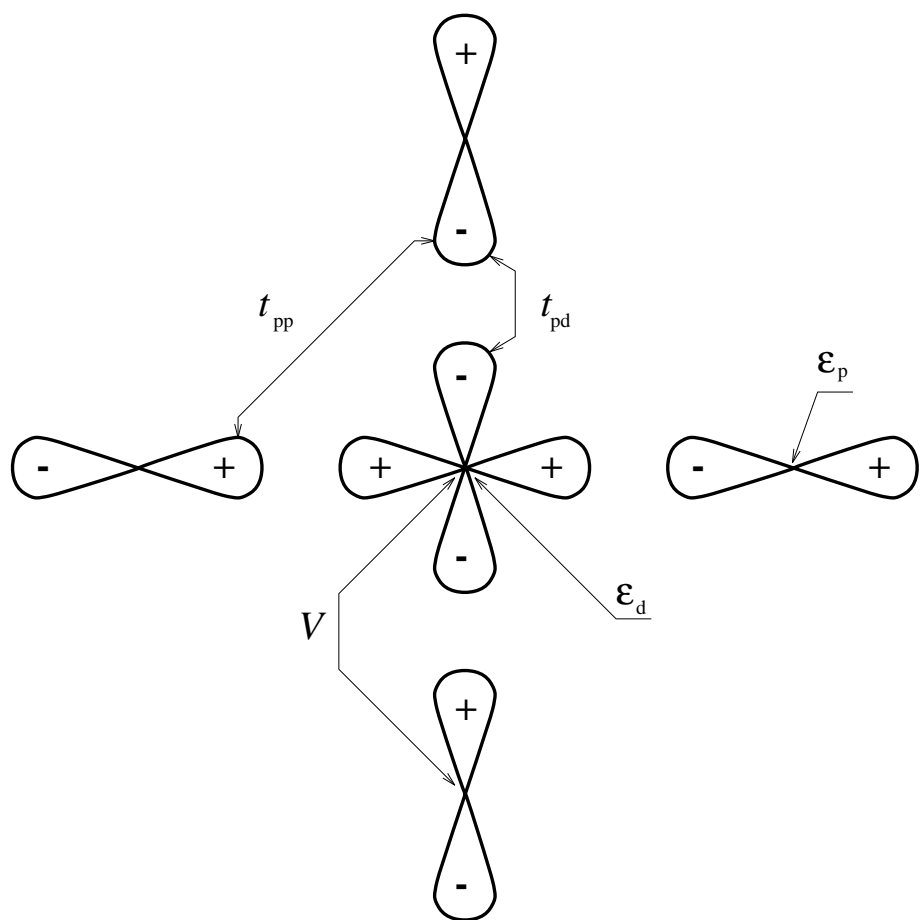
FIG. 1. The arrangement of copper d -orbitals and oxygen p -orbitals in the CuO_2 plane, with signs “+” and “-” accounting for the phase factors in the atomic wave functions, which result in the alternating signs of hopping terms in the tight-binding Hamiltonian.

FIG. 2. The phase diagrams for $t_{pd} = 1.3$ eV, $t_{pp} = 0.65$ eV, and $V = 1.25$ eV (a), and for $t_{pd} = 1.3$ eV, $t_{pp} = 0.8$ eV, and $V = 0.5$ eV (b). Notice the difference in the shapes of the heavy fermion (HF) region. The solid bold lines represent BRT, the dashed bold lines - a smooth crossover between HF and normal metal behaviour. The dotted line in fig. 3b corresponds to analytical result for the HF to normal metal crossover, obtained in the limit of small $n_0 - 1$.

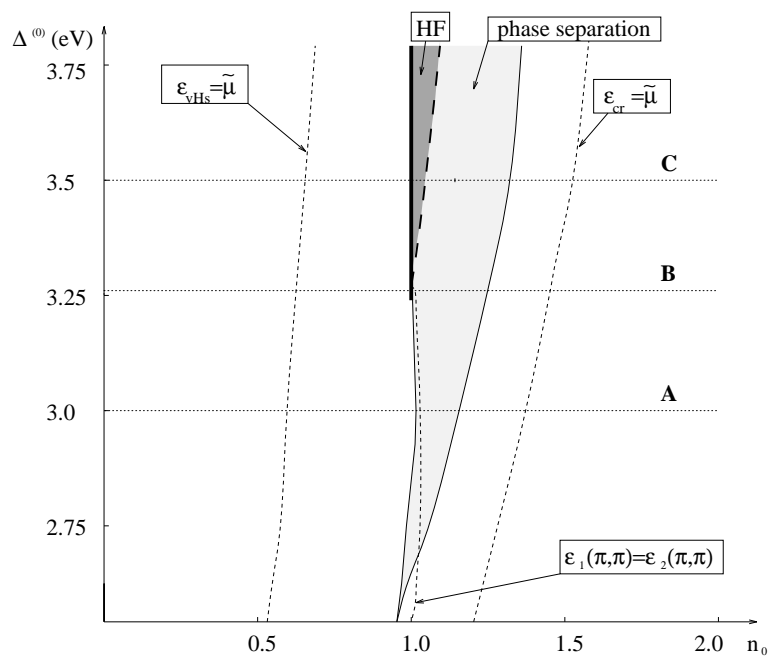
FIG. 3. The bandstructure energy scales: the bandwidth of the lowest band (solid lines), $\tilde{\mu} - \epsilon_{cr}$ (dashed lines), and $\tilde{\mu} - \epsilon_{vHs}$ (dotted lines), computed along the three cuts A, B, and C in fig. 2a.

FIG. 4. The Fermi surfaces for $n_0 = 1.23$ (dotted lines), $n_0 = 1.46$ ($n_0 \approx n_{cr}$, solid lines), and $n_0 = 1.64$ (dashed lines). The bare parameters of the system are $t_{pd} = 1.3$ eV, $t_{pp} = 0.65$ eV, $V = 1.25$ eV, and $\Delta^{(0)} = 3.26$ eV (cut B in fig. 2a), and the number 0, 1 and 2 indicate the number of filled bands in each region of the Brillouin zone.

FIG. 5. The rigid-band estimate for the interband term in the optical (ab)-plane conductivity ($\text{ohm}^{-1}\text{cm}^{-1}$) versus frequency (eV) at $n_0 = 1.44$, $t_{pd} = 1.3$ eV, $t_{pp} = 0.65$ eV, $V = 1.25$ eV, and $\Delta^{(0)} = 3.26$ eV. We used the value of 12 \AA for the interplane spacing.



(a)



(b)

